THE JOURNAL OF PHYSICAL CHEMISTRY A LETTERS

2007, *111,* 4727−4730
Published on Web 05/16/2007

Stability of the Hydrogen Trioxy Radical via Infrared Action Spectroscopy

Craig Murray, Erika L. Derro, Timothy D. Sechler, and Marsha I. Lester*

Department of Chemistry, University of Pennsylvania, Philadelphia, Pennsylvania 19104-6323

Received: February 21, 2007; In Final Form: March 12, 2007

The hydrogen trioxy radical (HO_3) has been proposed as an intermediate in several important chemical reactions and relaxation processes involving OH in the atmosphere. In this work, the gas-phase infrared action spectrum of HO_3 is obtained in the OH overtone region, along with the product state distribution of the OH fragment following dissociation. The highest observed OH product channel sets an upper limit for the $HO-O_2$ binding energy of 6.12 kcal mol^{-1}. The experimental stability of HO_3 and derived equilibrium constant imply that up to 66% of atmospheric OH may be converted into HO_3 in the tropopause region.

The existence of the hydrogen trioxy radical (HO_3 alternatively denoted HOOO) has several important implications in atmospheric chemistry, as it may act as an intermediate in key chemical reactions and relaxation processes in the atmosphere

$$H + O_3 \rightarrow OH\ (v \leq 9) + O_2 \qquad \text{(R1)}$$

$$OH\ (v) + O_2 \rightarrow OH\ (v - 1) + O_2 \qquad \text{(R2)}$$

$$O + HO_2 \rightarrow OH + O_2 \qquad \text{(R3)}$$

Emission from highly vibrationally excited OH produced by (R1) is responsible for the Meinel bands that dominate mesospheric airglow. Collisional deactivation by O_2 reaction (R2) is the major removal process, and it has been suggested that formation of the HO_3 complex controls the relaxation kinetics.[1] Isotopic-labeling studies have suggested that the mechanism for (R3), a key reaction in the atmospheric HO_x cycle, does not involve simple H-atom abstraction but rather occurs via an intermediate.[2] Furthermore, and perhaps most importantly, if HO_3 is stable relative to the $OH + O_2$ asymptote, it may act as a temporary sink for OH radicals and be present in measurable concentrations in the Earth's atmosphere.

Yet many of the properties of HO_3 remain elusive. Indeed, there has been much debate in the literature as to whether HO_3 is stable or metastable with respect to the $OH + O_2$ asymptote. In this report, we present the gas-phase infrared spectrum of HO_3, recorded in the OH stretch overtone region, and an upper limit to the dissociation energy, obtained by detection of the OH products following predissociation. In addition, statistical mechanical calculations of thermodynamic properties based on the measured stability as well as unimolecular dissociation kinetics and photolysis rates are used to assess the atmospheric importance of the HO_3 radical intermediate.

Empirically, the existence of HO_3 was confirmed by the neutralization/reionization work of Cacace et al.[3] and it has subsequently been observed by infrared spectroscopy in Ar and H_2O-ice matrices.[4,5] The most revealing information thus far comes from the Fourier transform microwave (FTMW) spectroscopy work of Suma et al.,[6] who measured the rotational spectrum and derived the structure of *trans*-HO_3. However, the stability of HO_3 remains the subject of considerable uncertainty. To date, the only experimental measurement of the stability of HO_3 is indirect; Speranza inferred 10 ± 5 kcal mol^{-1} from a comparison of the electron-transfer efficiency of HO_3^+ with a series of neutrals.[7] However, this value is in marked disagreement with most theory, and the interpretation of the experimental data has been questioned by Denis et al.[8] whose recommended enthalpy of formation implies a stability of only 1.8 kcal mol^{-1}, while more recent calculations, for example, by Fabian et al.[9] suggest 1.1−3.9 kcal mol^{-1}.

Ab initio calculations of the structure and stability of HO_3 are, in general, strongly dependent on both the method and the size of the basis set, and consequently are highly variable.[8,10−12] There is consensus that HO_3 is planar but not whether the cis or trans conformer is more stable. Furthermore, it has been suggested[6] that single-reference methods, which have been used in the majority of theoretical studies, provide an inadequate description of HO_3 electronic structure and that a multireference treatment is required even to obtain an accurate geometry. The major failing of single reference methods is an artificially short central O−O bond when compared with $r_{O-O} = 1.688$ Å determined from microwave spectroscopy;[6] the bond length is typically underestimated by up to 0.3 Å. To date, the highest level geometry optimization reported is MRCI+Q/aug-cc-pVTZ by Suma et al.[6] who find *trans*-HO_3 to be marginally more stable than *cis*-HO_3 with $r_{O-O} = 1.677$ Å and $D_e = 3.90$ kcal mol^{-1}.

In the present experiments, HO_3 radicals are readily produced by the association of O_2 and OH radicals generated by photolysis of nitric acid in the collisional region of a supersonic free-jet expansion of 20% O_2 in Ar. Tunable infrared radiation at ∼1.4 μm, generated by an optical parametric oscillator, is used to excite the first OH overtone transition in HO_3, causing dissociation to OH and O_2; then, a frequency doubled dye laser probes the OH products by saturated laser-induced fluorescence (LIF), as illustrated in Figure 1. The spatially overlapped IR and UV laser beams intersect the expansion approximately

* Author to whom all correspondence should be addressed: E-mail: milester@sas.upenn.edu. Phone: (215) 898-4640. Fax: (215) 573-2112.

10.1021/jp071473w CCC: $37.00

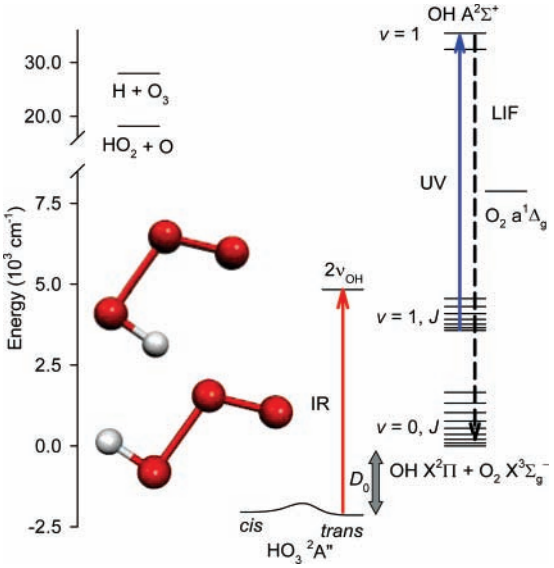

Figure 1. Energy level diagram illustrating HO_3 as an intermediate in $HO_2 + O$, $H + O_3$, and $OH + O_2$ reactions. The binding energy of *trans*-HO_3 is derived from this work and shown relative to $OH + O_2$ products. The relative energy of the *cis*-HO_3 conformer and the isomerization barrier are taken from calculated values.[6] The experimental approach is also illustrated schematically. IR excitation in the OH stretch overtone region ($2\nu_{OH}$) causes HO_3 to predissociate and the nascent OH products are subsequently probed by UV LIF.

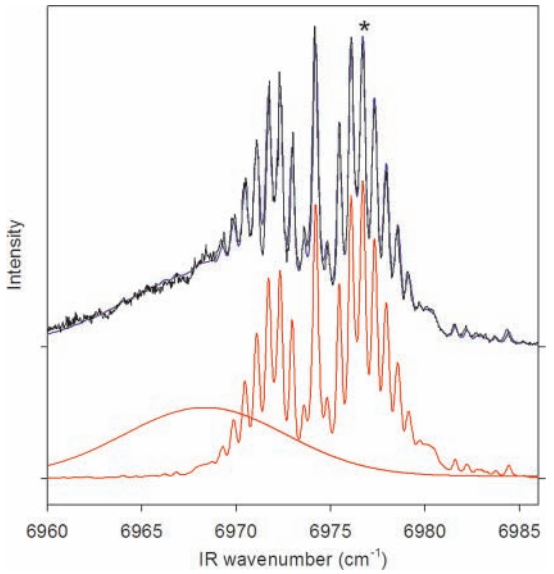

Figure 2. Infrared action spectrum of HO_3 at 9 K in the $2\nu_{OH}$ region. The simulation (red) is comprised of two distinct features: (A) a rotationally structured band with vibrational band origin at 6974.18(5) cm^{-1} simulated using experimental rotational constants for *trans*-HO_3 and (B) a broad feature represented by a Lorentzian line profile centered at ~6967 cm^{-1}.[6] The sum of the two simulations (blue) is superimposed on the experimental spectrum (black), which is offset vertically. The infrared action spectrum was recorded with the UV fixed on the OH A−X (1,1) $P_1(4)$ transition. The asterisk at 6976.7 cm^{-1} indicates the IR transition used to measure the OH product state distribution.

$x/D = 15$ nozzle diameters downstream ~20 μs after photolysis and thus probe rotationally cold HO_3 radicals.

The IR action spectrum of HO_3 in the OH stretch overtone region from 6960 to 6986 cm^{-1} is shown in Figure 2. The spectrum was recorded with the UV laser fixed on the OH A−X (1,1) $P_1(4)$ transition but was unchanged, except in intensity, irrespective of the choice of probe transition. There are two distinct features in the infrared action spectrum: (A) a rotationally structured band with vibrational origin at 6974.18(5) cm^{-1} and (B) a broad feature centered ~7 cm^{-1} lower in energy. Scanning the infrared laser to both lower and higher energy regions (±250 cm^{-1}) revealed no other features in the action spectrum. The line positions and intensities of feature (A) are very well reproduced by a simulation using the *trans*-HO_3 rotational constants ($r_{O-O} = 1.688$ Å) from the FTMW work of Endo and co-workers[6] and a rotational temperature of 9 K; simulations based on theoretically predicted structures for *trans*-HO_3 with shorter central O−O bonds[8,9] give noticeably poorer agreement. A simulation using rotational constants for *cis*-HO_3 from a multireference calculation[6] also showed significantly poorer agreement. As such, we assign the rotationally structured band to the OH overtone of *trans*-HO_3. The spectrum displays a homogeneously broadened Lorentzian line width of 0.20 cm^{-1}, corresponding to a 27 ps lifetime for the vibrationally excited-state due to intramolecular vibrational redistribution and/or predissociation. The distinct P-, Q-, and R-branch structure in the *trans*-HO_3 spectrum is characteristic of a predominantly *a*-type transition, while a small *b*-type component (*a*/*b* ratio of 5:1) contributes to structure in the wings of the spectrum.

In contrast, the identification of feature (B) in the IR action spectrum is more problematic. The OH product state distributions are similar following excitation on the structured or the broad feature suggesting that the absorbing species are chemically similar and that the integrated intensity ratio of (A)/(B) = 1.6:1 will be a reasonable measure of the relative populations, assuming similar absorption cross sections. The sum of the broad and structured simulations is shown as an overlay in the top trace of Figure 2. The infrared action spectrum was recorded for DO_3 in a manner comparable to the one described previously, replacing OH with OD radicals. The DO_3 overtone spectrum exhibits qualitatively the same features: a rotationally structured band with origin at 5182.42(5) cm^{-1} and a broad feature centered ~6 cm^{-1} to lower energy. As with HO_3, the rotationally structured band was better simulated using FTMW rotational constants for the trans conformer.[6] The presence of an analogous broad, unstructured feature in the DO_3 spectrum precludes the possibility of its origin being an excitation to a repulsive electronic state.

One possibility is that the broad feature is the *cis*-HO_3 conformer, even though at first glance this seems unlikely because ab initio frequency calculations predict the overtone to be red-shifted by ~100 cm^{-1} as a consequence of an interaction between the terminal oxygen and the hydrogen atoms. However, the predicted spectral shift for *cis*-HO_3 is derived from single reference methods that yield a shorter central O−O bond for both conformers than is supported by the spectroscopic data for *trans*-HO_3. A longer central O−O bond for *cis*-HO_3 may suggest a weaker intramolecular interaction, which would in turn lead to a smaller red shift and bring the *cis*-HO_3 overtone closer to that of *trans*-HO_3. This would be consistent with an analogous broad feature in the DO_3 overtone spectrum, as the isotopic shifts are expected to be similar for both conformers. If the broad feature is due to absorption by *cis*-HO_3, the absence of rotational structure could be explained by fast isomerization to *trans*-HO_3 followed by dissociation. This would suggest a smaller binding energy for *cis*-HO_3, consistent with the integrated intensity ratio. In this case, the broad feature can be represented by a lifetime-broadened (5.0 cm^{-1}, 1 ps lifetime) simulation using calculated *cis*-HO_3 rotational constants.[6]

The nascent OH $X^2\Pi_\Omega$ product state distribution following dissociation of *trans*-HO_3 was recorded by fixing the IR laser

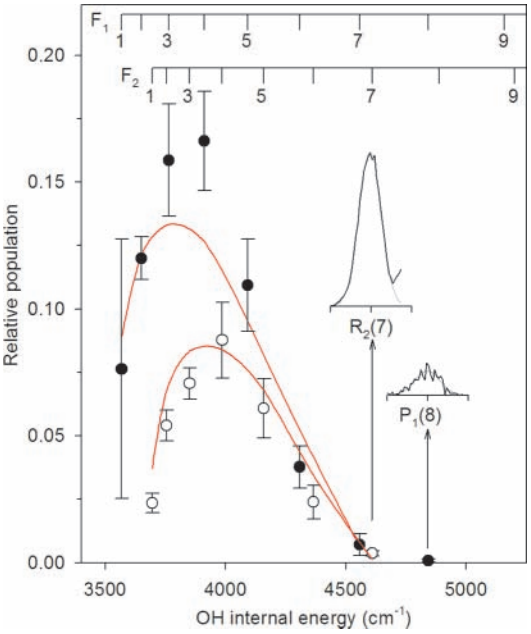

Figure 3. Rotational state distributions of OH $X^2\Pi_\Omega$, $v = 1$ in the F_1 $\Omega = 3/2$ (closed circles) and F_2 $\Omega = 1/2$ (open circles) spin−orbit manifolds following overtone excitation of *trans*-HO_3 at 6976.7 cm^{-1}. The error bars represent 2σ uncertainties. The insets show the experimental LIF spectra recorded on the $R_2(7)$ and $P_1(8)$ transitions of the OH A−X (1,1) band, the latter indicating population in the F_1, $N = 8$, *e* level with an internal energy of 4840.2 cm^{-1}. The red lines are statistical prior distributions calculated with the constraint that the OH population is produced in $v = 1$ from which a binding energy of 2260 ± 30 cm^{-1} or 6.46 ± 0.09 kcal mol^{-1} is derived. The highest energy OH state observed lies beyond the cut off of the prior distributions, and consequently we prefer the upper limit to D_0 defined by simple energy conservation.

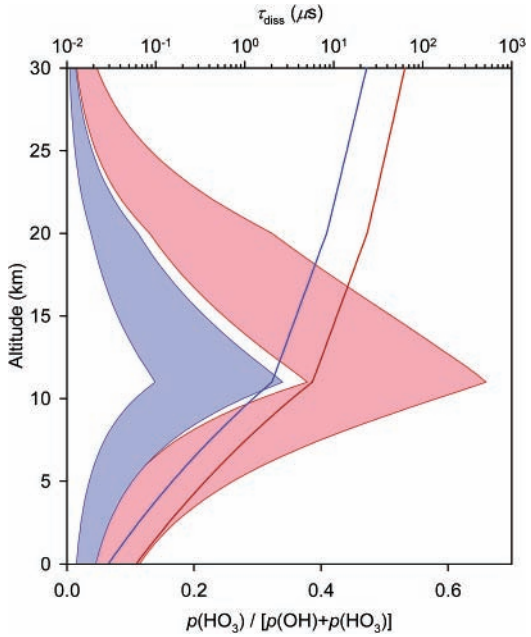

Figure 4. The fraction of atmospheric OH predicted to be found as HO_3 as a result of the equilibrium OH + O_2 + M ⇌ *trans*-HO_3 + M displayed as a function of altitude, calculated using both the upper limit D_0 of 2140 cm^{-1} (pale red region) and an arbitrarily reduced D_0 of 1940 cm^{-1} (pale blue region). The lower edges arise from treatment of all *trans*-HO_3 vibrational modes as harmonic oscillators while the upper edges treat the lowest frequency mode (torsion about the central O−O bond) as a free rotor. The lifetime of *trans*-HO_3 with respect to unimolecular dissociation, τ_{diss}, calculated treating all vibrational modes as harmonic oscillators, is also displayed for the same values of D_0 as the solid red and blue lines.

on the R(3) transition of the overtone band at 6976.7 cm^{-1}, selected to minimize contribution from the broad feature that underlies the structured spectrum, and scanning the UV laser over various OH A−X transitions. Population was observed in $v = 1$ but not $v = 0$. The OH $X^2\Pi_\Omega$, $v = 1$ rotational state distributions, normalized to unity after summing over Λ-doublets, in both the F_1 and F_2 spin−orbit manifolds are displayed in Figure 3. A propensity for the Π(A′) Λ-doublet was observed, but will not be discussed here. An upper limit for D_0 can be obtained straightforwardly from conservation of energy and a measurement of the highest energetically open OH quantum state,[13] OH $X^2\Pi_{3/2}$, $v = 1$, $N = 8$, *e* at 4840.2 cm^{-1}, giving $D_0 \leq 2140$ cm^{-1} or 6.12 kcal mol^{-1}.[14] This allows the calculation of a lower limit for the enthalpy of formation of $\Delta_f H$ (298.15 K) ≥ 1.7 kcal mol^{-1} for HO_3, using the current recommended[15] value for OH and standard thermal corrections. Our value for the enthalpy of formation agrees within the considerable uncertainty limits reported in the only previous indirect experimental determination of −1 ± 5 kcal mol^{-1} [7] and provides an important refinement by constraining it to be positive.

The experiments described are blind to the product state distribution in the O_2 fragment, and consequently the upper limit to the dissociation energy assumes negligible contribution from its internal states and translational recoil. In principle, the infrared photon provides sufficient energy to populate O_2, $v = 1$ in conjunction with the highest open OH, $v = 1$ state, which would reduce the upper limit for D_0 to 584 cm^{-1} or 1.67 kcal mol^{-1}. However, this scenario yields an unreasonably small binding energy, given the central O−O bond length of HO_3. Considering the analogous molecules FO_2 and ClO_2, the central O−O bond in HO_3 is intermediate to the F−O and Cl−O bonds ($r_{F-O} = 1.65$ Å and $r_{Cl-O} = 2.08$ Å), although far closer to the former.[16,17] It is therefore likely that the binding energy of HO_3 would also be intermediate to that of FO_2 and ClO_2, which are $D_0 = 9.0$ and 4.7 kcal mol^{-1}, respectively,[18,19] indicative of chemical bond formation rather than a purely electrostatic attraction. It is noteworthy that the dipole−quadrupole interaction would contribute only 40−140 cm^{-1} to the binding energy in the most favorable linear OH···OO orientation at typical van der Waals distances of ∼3−4 Å.

We apply a standard statistical mechanical approach[20] to derive the equilibrium constant, $K_p(T)$, for the OH + O_2 + M ⇌ HO_3 + M association reaction (with collision partner M) based on our upper limit for D_0 and subsequently to calculate the fraction of atmospheric OH expected to exist in the form of HO_3. Free energies of all species were calculated within the rigid rotor, harmonic oscillator approximation using known molecular constants[6,21] and previously calculated[9] harmonic vibrational frequencies for *trans*-HO_3. The lowest frequency mode, torsion about the central O−O bond, was treated as a harmonic oscillator or alternatively as a free rotor, the latter approach increasing the entropic contribution to the free energy[22] and driving the equilibrium further toward products. Through the use of the harmonic oscillator (free rotor) approach, the calculated $K_p(T)$ is 0.13 (0.42) atm^{-1} at 298 K, and increases with decreasing temperature. At a typical tropopause temperature of 210 K, K_p is 23.1 (73.9) atm^{-1} strongly favoring the production of HO_3. As shown in Figure 4, the thermodynamic calculations imply that the partial pressure of HO_3 should peak in the vicinity of the tropopause and may account for up to 66% of atmospheric OH. The predicted HO_3 partial pressure decreases to both lower and higher altitudes as a consequence of increasing temperature and decreasing pressure, respectively,

but remains a significant fraction of the total OH. The magnitude of $K_p(T)$ is, however, strongly dependent on binding energy. Figure 4 also shows the effect on the HO_3 concentration for an arbitrary decrease of only 200 cm^{-1} in D_0, which is accompanied by a fourfold decrease in K_p at 210 K, highlighting the importance of accurate measurements of this quantity.

Within the atmosphere there exist three primary loss processes that determine the kinetic stability of HO_3: unimolecular decomposition, photodissociation, and reaction. At present, little is known about reactive properties of HO_3, except that it is predicted to be further stabilized by complexation with water.[23] Photochemically, infrared absorption in the overtone and, in principle, the fundamental OH stretch regions regenerate OH and O_2 with a quantum yield of unity. Consideration of the average solar radiance in these spectral regions and estimated absorption cross sections suggest a lifetime of ~1 daylight hour if combination bands are neglected. Clearly, the presence of other abundant and strong absorbers, such as H_2O and CO_2, will serve to reduce the actinic photon flux and therefore increase further the photochemical lifetime. Conversely, a predicted visible absorption at ~550 nm, where the solar radiance is significantly larger, to the dissociative $^2A'$ state[24] may have a significant impact on the photochemical removal rate. Finally, the rate of unimolecular decomposition can be assessed using the theoretical formalism provided by Troe.[25−27] The Lennard-Jones collision parameters for HO_3 were approximated by those for HO_2 and the collision partner was air.[28] Vibrational frequencies were again taken from Fabian et al.[9] Figure 4 shows the resultant strong collision lifetimes for HO_3 as a function of altitude. The lifetime is found to be on the order of microseconds above ~6 km and is approximately a factor of 2 smaller than that calculated for the analogous ClO_2 molecule, consistent with the establishment of a rapid equilibrium between OH and O_2.

From a fundamental chemical viewpoint, the hydrogen trioxy radical and its halogenated analogs[6,18] provide a challenge to contemporary theory requiring the application of high level ab initio methods for accurate calculation of geometry and stability. Perhaps more importantly, the upper limit for D_0 of 6.12 kcal mol^{-1} measured in these HO_3 experiments has potentially profound implications for atmospheric chemistry, for which the reactivity of the OH radical is of central importance. Its stability supports the likely role of HO_3 as an intermediate in key atmospheric processes (R1−R3). Thermodynamic and kinetic considerations imply the establishment of a rapid equilibrium $OH + O_2 + M \rightleftharpoons HO_3 + M$ that is finely balanced between OH reactants and HO_3 products in the vicinity of the tropopause. Our results strongly suggest that HO_3 will exist in the atmosphere in significant and possibly measurable quantities, and that investigation of its chemical reactivity is highly desirable with a view to inclusion of this equilibrium in atmospheric chemistry models.

Acknowledgment. We thank Mark D. Marshall and Yasuki Endo for sharing unpublished theoretical calculations. This work was supported by the Chemistry Division of the National Science Foundation. C.M. acknowledges financial support from the Dreyfus Postdoctoral Program in Environmental Chemistry.

References and Notes

(1) McCabe, D. C.; Smith, I. W. M.; Rajakumar, B.; Ravishankara, A. R. *Chem. Phys. Lett.* **2006**, *421*, 111.

(2) Sridharan, U. C.; Klein, F. S.; Kaufman, F. *J. Chem. Phys.* **1985**, *82*, 592.

(3) Cacace, F.; De Petris, G.; Pepi, F.; Troiani, A. *Science* **1999**, *285*, 81.

(4) Nelander, B.; Engdahl, A.; Svensson, T. *Chem. Phys. Lett.* **2000**, *332*, 403; (Erratum) *Chem. Phys. Lett.* **2001**, *339*, 295.

(5) Cooper, P. D.; Moore, M. H.; Hudson, R. L. *J. Phys. Chem. A* **2006**, *110*, 7985.

(6) Suma, K.; Sumiyoshi, Y.; Endo, Y. *Science* **2005**, *308*, 1885.

(7) Speranza, M. *Inorg. Chem.* **1996**, *35*, 6140.

(8) Denis, P. A.; Kieninger, M.; Ventura, O. N.; Cachau, R. E.; Diercksen, G. H. F. *Chem. Phys. Lett.* **2002**, *365*, 440; (Erratum) *Chem. Phys. Lett.* **2003**, *377*, 483.

(9) Fabian, W. M. F.; Kalcher, J.; Janoschek, R. *Theor. Chem. Acc.* **2005**, *114*, 182.

(10) Jungkamp, T. P. W.; Seinfeld, J. H. *Chem. Phys. Lett.* **1996**, *257*, 15.

(11) Setokuchi, O.; Sato, M.; Matuzawa, S. *J. Phys. Chem. A* **2000**, *104*, 3204.

(12) Yu, H. G.; Varandas, A. J. C. *Chem. Phys. Lett.* **2001**, *334*, 173.

(13) The energy balance equation is $E_{int}(HO_3) + h\nu_{IR} - D_0 = E_{int}(OH) + E_{int}(O_2) + KE$. The internal energy of HO_3, $E_{int}(HO_3)$, is known from the lower level of the overtone transition used for excitation and correspondingly the infrared photon energy, $h\nu_{IR}$. With the assumption that the internal energy of O_2, $E_{int}(O_2)$, and the kinetic energy release, *KE*, are negligible, measurement $E_{int}(OH)$ determines the maximum possible D_0.

(14) Colin, R.; Coheur, P.-F.; Kiseleva, M.; Vandaele, A. C.; Bernath, P. F. *J. Mol. Spectrosc.* **2002**, *214*, 225.

(15) Ruscic, B.; Boggs, J. E.; Burcat, A.; Császár, A. G.; Demaison, J.; Janoschek, R.; Martin, J. M. L.; Morton, M. L.; Rossi, M. J.; Stanton, J. F.; Szalay, P. G.; Westmoreland, P. R.; Zabel, F.; Bérces, T. *J. Phys. Chem. Ref. Data* **2005**, *34*, 573.

(16) Yamada, C.; Hirota, E. *J. Chem. Phys.* **1984**, *80*, 4694.

(17) Suma, K.; Sumiyoshi, Y.; Endo, Y. *J. Chem. Phys.* **2004**, *121*, 8351.

(18) Feller, D.; Dixon, D. A. *J. Phys. Chem. A* **2003**, *107*, 9641.

(19) Suma, K.; Sumiyoshi, Y.; Endo, Y.; Enami, S.; Aloisio, S.; Hashimoto, S.; Kawasaki, M.; Nishida, S.; Matsumi, Y. *J. Phys. Chem. A* **2004**, *108*, 8096.

(20) Vaida, V.; Headrick, J. E. *J. Phys. Chem. A* **2000**, *104*, 5401.

(21) *NIST Chemistry WebBook, NIST Standard Reference Database Number 69*; Lindstrom, P. J., Mallard, W. G., Eds.; NIST: Gaithersburg, MD, 2005.

(22) East, A. L. L.; Radom, L. *J. Chem. Phys.* **1997**, *106*, 6655.

(23) Aloisio, S.; Francisco, J. S. *J. Am. Chem. Soc.* **1999**, *121*, 8592.

(24) Yang, J.; Li, Q. S.; Zhang, S. *Phys. Chem. Chem. Phys.* **2007**, *9*, 466.

(25) Troe, J. *J. Chem. Phys.* **1977**, *66*, 4758.

(26) Troe, J. *J. Chem. Phys.* **1977**, *66*, 4745.

(27) Troe, J. *J. Phys. Chem.* **1979**, *83*, 114.

(28) Hirschfelder, J. O.; Curtiss, C. F.; Bird, R. B. *Molecular Theory of Gases and Liquids*; John Wiley & Sons, Inc.: New York, 1967.